Dissimilar Lap Welding of Ni-based Metallic Glass and Stainless Steel Foil by Fiber Laser Beam†

TSUMURA Takuya *, HAMADA Shinsuke **, KIMURA Hisamichi *, INOUE Akihisa**** and NAKATA Kazuhiro*******

Abstract

Dissimilar joining of $Ni_{60}Nb_{15}Ti_{15}Zr_{10}$ metallic glass foils to type316L stainless steel foils has been investigated using a fiber laser welding method. Dissimilar joints without cracking were obtained at the condition of laser power from 20 W to 35 W with constant welding speeds of 100 mm/s and argon gas shielding. Partial crystallization of metallic glass weld was detected by XRD over 30 W of laser power. Fracture loads of dissimilar joints increased with increasing laser power, but excess laser power at 35 W reduced the joint strength due to crystallization of the welds.

KEY WORDS: (Ni-based metallic glass foil), (Stainless steel foil), (Laser welding), (Fiber laser), (Tensile shear test)

1. Introduction

Ni-based metallic glasses, Ni-Zr-Ti-(Si, Sn)[1], Ni-Nb-Ti-Zr-Co-Cu[2], Ni-Nb-Ti-Zr[3], Ni-Nb-Ti[4], Ni-Nb-Sn[5] and some other systems, were developed in the early 2000's. These exhibited comparably higher compressive strength than the Zr- and Pd- based metallic glasses[2-4]. Among them, Ni-Nb-Ti-Zr foil has been expected to apply to the separator of the proton exchange membrane fuel cell[6] and various precision machinery components, because it has also high corrosion resistance and high viscous flow ability. However, the critical width of their foils is limited to 50 mm of a ribbon shape, because they are produced by melt-spinning techniques. Therefore, making them with a large size is indispensable for practical use. Furthermore, dissimilar metal joining of metallic glasses are necessary to use them as an industrial material.

It is reported that Ni-Nb-Ti-Zr-Co-Cu metallic glass foil was successfully welded together by fiber laser welding and the weld bead consisted of only the amorphous state[7-9]. Moreover, $Zr_{55}Al_{10}Ni_5Cu_{30}$ metallic glass 2 mm-thick sheet was welded by fiber laser beam at ultra-high-welding speed without crystallization[10] because of relatively-high cooling rate in the weldment and HAZ caused by a tightly focused fiber laser beam with comparatively-high energy density than any other laser heat sources. In this study, therefore, we welded $Ni_{60}Nb_{15}Ti_{15}Zr_{10}$ metallic glass foils to type316L stainless steel foil, (which is a typical corrosion-resistant industrial material and is also used in fuel cells,) by using fiber laser welding in order to make a dissimilar metal joint.

2. Experimental

An ingot of the $Ni_{60}Nb_{15}Ti_{15}Zr_{10}$ alloy was prepared by arc-melting the mixture of pure elements in an argon atmosphere. From this ingot, a metallic glassy ribbon of 50 mm in width and 35 μm in thickness was produced by using single-roller melt-spinning equipment. Commercially available type316L stainless steel foil of 30 μm in thickness was used as a counter material. Width and length of each specimen was 5 mm and 30 mm, respectively, and the surface was cleaned with absolute ethanol just after the test. Upper $Ni_{60}Nb_{15}Ti_{15}Zr_{10}$ metallic glass (BMG) foil was stacked on lower type 316L stainless steel (Type316L) foil with the overlap space of 10 mm. During welding, the specimen was fixed by a magnet holder on a backing plate, and a laser beam irradiated on the surface of BMG foil, which had contact with the single-roll when the foil was made by melt-spinning technique. The fiber laser welding was carried out in argon gas shielding of 15 *l*/min using a fiber laser welder (SPI Lasers Co. Ltd. SP100C) with a maximum power of 100 W and laser spot diameter of 50 μm. The laser power was varied from 15 W to 40 W

† Received on December 26, 2011
* Assistant Professor
** Graduate Student (currently Nissan Motor Co., Ltd.)
*** Associate Professor, IMR, Tohoku University
**** Professor, Tohoku University
***** Professor
Transactions of JWRI is published by Joining and Welding Research Institute, Osaka University, Ibaraki, Osaka 567-0047, Japan

with the constant welding speed of 100 mm/s.

Some of the welded samples were mounted by conductive epoxy resin, cured at 180 °C for about 15 min, and ground by SiC paper #120 - #1200, polished by 3.0 µm and 1.0 µm polycrystalline diamond to provide micro-structural information. During metallographic examination, the welded samples were etched by electrolytic etching at 8 V for 10 s to 30 s with 10 % oxalic acid solution and cathode electrode of type-304 stainless steel. Microstructure of welded specimens was investigated by using optical microscopy (KEYENCE Co. Ltd. VHX-200), scanning electron microscopy (Hitachi High-Technologies Co. Ltd. SU-70), and micro-area X-ray diffractometry (Bruker AXS Co. Ltd. D8: CoKα). Mechanical properties of the welded joint were measured by tensile share test, which was performed by using an Instron 5500R with the crosshead speed of 0.5 mm/min.

3. Results and Discussion

Laser welding of dissimilar metals has been achieved at the conditions of different laser powers from 20 W to 35 W for a constant welding speed of 100 mm/s. At the laser power of 15 W, $Ni_{60}Nb_{15}Ti_{15}Zr_{10}$ BMG foil was not joined to Type316L foil, and at the laser power of 40 W, both BMG and Type316L foils were melt-through and cut by laser beam.

Figure 1 shows the appearances of weld bead surface and cross sections of as-polished and etched conditions at each laser power. Here, the appearance of top BMG surface only shows in the figure because weld bead was not observed at the bottom surface of Type316L foil. Defects and cracks were not observed on the weld bead surfaces and cross sections within these laser powers. All weld beads were smooth and they seem to consist of only HAZ-2 zone, which was observed under bead-on-plate diode laser welding[7]. This fact indicates that the weld bead near the surface is almost kept in an amorphous state or partially crystallized phase. From the cross-sectional view in as-polished samples of Fig. 1, gap or etched region was not seen in the BMG foil and at the welded interface between upper BMG foil and lower Type316L foil. However, from the cross section after etching, the welded interfaces appear with thin dark layers when the laser power is 30 W or lower and the thin gauche dark layer was formed into the BMG side when the laser power is 35 W.

Figure 2 shows SEM and EDX images on the cross section of the BMG / Type316L weld interface. EDX analysis was carried out for the elements Ni, Ti, Nb, and Zr which are the components of BMG foil, and Fe and Cr which are the main components of Type316L foil. As shown in Fig. 2 (a), the lower Type316L foil was not melted and the component elements of BMG and Type316L were not mixed with each other. Therefore, it is suggested the melted BMG was only spread like at brazing filler metal on the lower Type316L surface and then the two foils were joined to each other at the welding condition under a laser power of 30 W. On the other hand, the gauche dark layer of the BMG side was

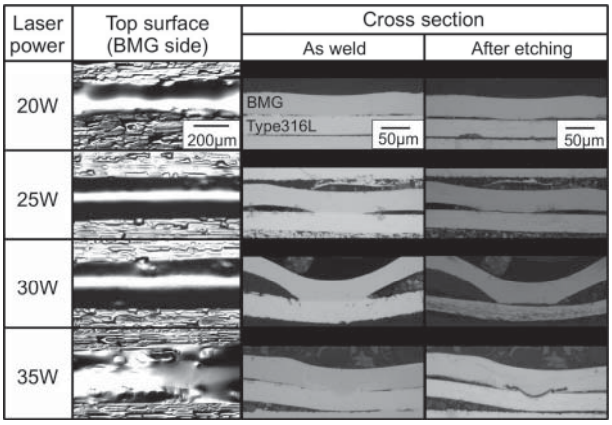

Fig. 1 Appearance and cross sections of weld bead by fiber laser welding at different powers.

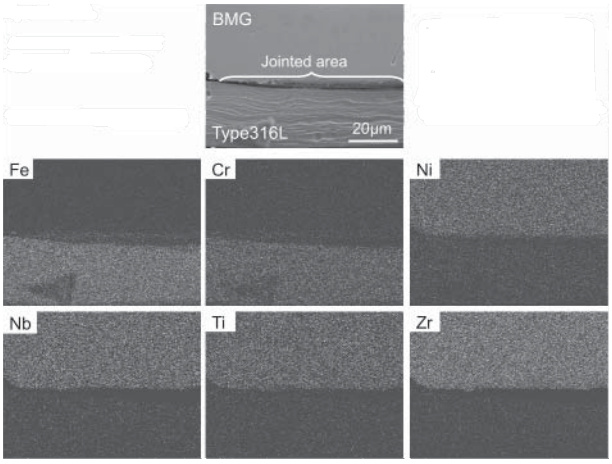

(a) Laser power: 30 W

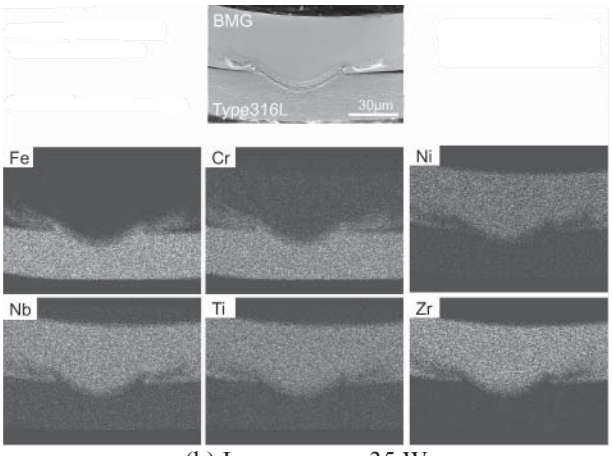

(b) Laser power: 35 W

Fig. 2 SEM and EDX images on cross section of weld bead by fiber laser welding.

formed by Fe and Cr elements, which are the component elements of Type316L foil as shown in Fig. 2 (b).

The micro-area XRD patterns taken from the weld bead surface in the center of the weld bead width and base metal are shown in **Fig. 3**. Here, the collimator size of 0.1 mm is larger than the weld bead width. Therefore, obtained patterns shown in Fig. 3 include the effect of

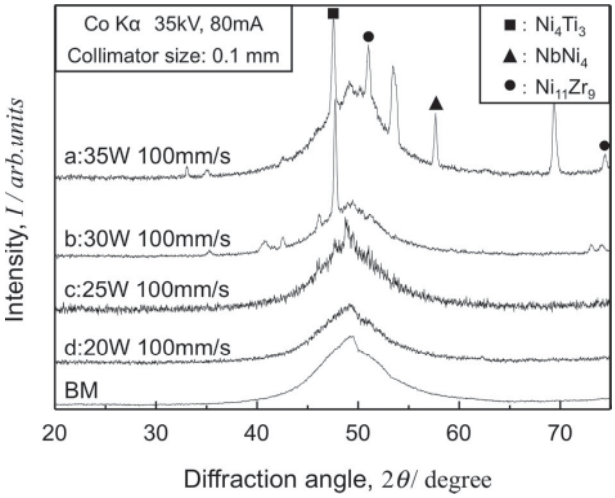

Fig. 3 X-ray diffraction patterns of weld bead surface and base metal.

both the weld bead and the heat-affected zone. From these diffraction patterns, some sharp peaks that suggest partial crystallization of metallic glass were observed at laser powers of 30 W or more. These peaks were indexed as Ni_4Ti_3, $NbNi_4$, and $Ni_{11}Zr_9$. However, at laser power of 25 W or less, the diffraction pattern showed about the same as base metal, which suggested the weld beads were not crystallized.

Figure 4 shows the result of tensile shear tests of the joint for each laser power. The fracture load shown in the vertical axis is the maximum load divided by the specimen width of 5 mm and that of the base metal is the value converted from their tensile strength. There were two fracture modes observed for the tensile shear test; one is broken at Type316L/BMG interface as shown in **Fig. 5** (a) and the other is broken at WM/HAZ in BMG side as shown in Fig. 5 (b). Fracture mode changed Type316L/BMG interface fracture to WM/HAZ in BMG side fracture with increasing laser power. Average fracture load increased with increasing laser power up to 30 W, but decreased at 35 W.

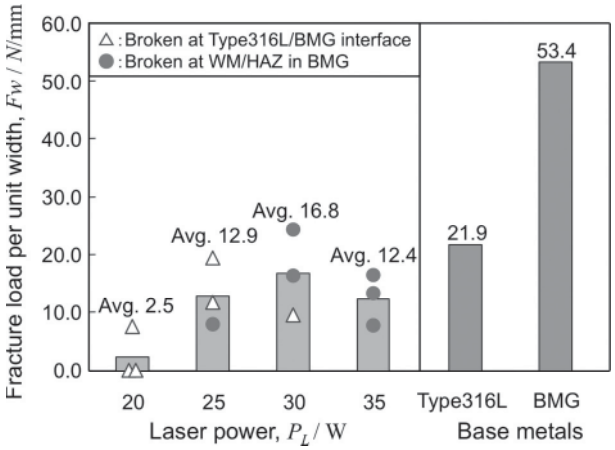

Fig. 4 Fracture load measured by tensile shear test of BMG/Type316L dissimilar lap welded joint at different laser powers comparing with tensile strength of base metals.

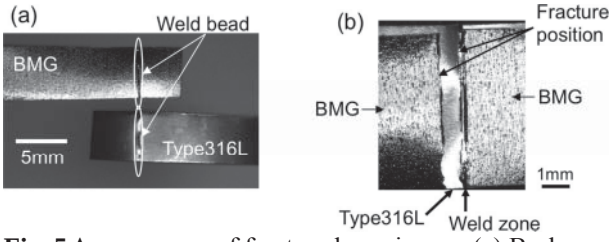

Fig. 5 Appearances of fractured specimens; (a) Broken at Type316L/BMG interface (laser power of 25 W), (b) Broken at WM/HAZ in BMG (laser power of 35 W).

Figure 6 shows SEM images of fracture surfaces of metallic glass sides. From these images, it can be seen that the width of the fractured area (w_f) increased with increasing laser power. **Figure 7** shows the relation between w_f and fracture load. It should be noticed that the increase of fracture load is attributed to the increase in w_f. At the laser power of 35 W, despite w_f increasing, fracture load decreased. This decrease seems to be attributed to the advanced partial crystallization of BMG in welded zone.

Figure 8 shows SEM and EDX images on fractured surfaces at laser power of 20 W. In this analysis, components of Type316L are detected on the fractured surface and not mixed with those of metallic glass. From this result, Type316L/BMG interface fracture was actually occurring at the interface of a lap joint between them with no obvious compound. This result suggests that the joint was formed mainly by wetting of metallic glass to Type316L.

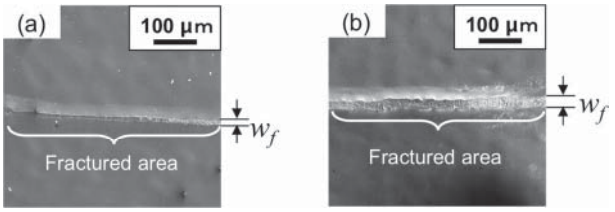

Fig. 6 SEM images of fractured surface of BMG side on the laser welded joint; Laser powers: (a) 20 W and (b) 25 W, w_f: Width of fractured area.

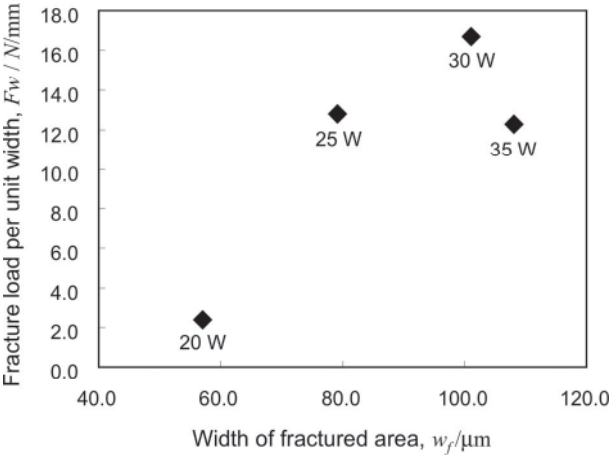

Fig. 7 Relationship between width of fractured area and fracture load.

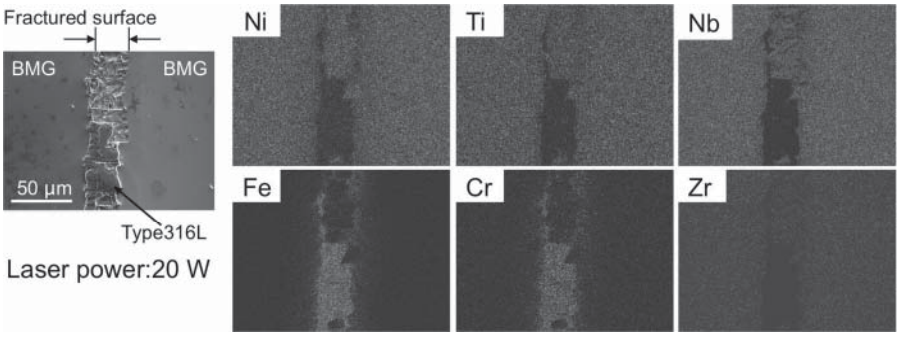

Fig. 8 SEM and EDX images on fractured surfaces of BMG side of laser welded joint with laser power of 20 W.

4. Summary

The dissimilar lap joint of Ni-based metallic glass and type316L stainless steel foils was obtained successfully and metallic glass was kept a non-crystalline structure at the welding condition of laser input of 20 W and 25 W with constant welding speeds of 100 mm/s. The strength of the joint increased with increasing laser power as the increase in the welded area, but the strength of the joint decreased at 35 W due to the progress of crystallization of metallic glass welds.

Acknowledgment

This research was supported by The Ministry of Education, Cultures, Sports, Science and Technology (MEXT) of Grant-in-Aid for Scientific Research on Priority Areas 428 KAKENHI (16039211 and 18029013), and was carried out by The Development Basis of Joining Technology for Metallic Glasses and Inorganic Materials (DBJT). We are also deeply grateful to Associate Prof. Kawahito and Prof. Katayama whose supports of use of the SP100C fiber laser welder for our study.

References

1) S. Yi, T. G. Park and D. H. Kim, *J. Mater. Sci.*, **15** (2000) 2425-2430.
2) T. Zhang and A. Inoue: *Mater. Trans.*, **43** (2002) 708-711.
3) A. Inoue, W. Zhang and T. Zhang: *Mater. Trans.*, **43** (2002), 1952-1956.
4) W. Zhang and A. Inoue: *Mater. Trans.*, **43** (2002) 2342-2345.
5) H. Choi-Yim, D. Xu and W. L. Johnson: *Appl. Phys. Lett.*, **82** (2003) 1030-1032.
6) A. Inoue, T. Shimizu, S. Yamaura, Y. Fujita, S. Takagi and H. Kimura,: *Mater. Trans.*, **46** (2005) 1706-1710.
7) T. Tsumura, K. Kobayashi, K. Nakata, N. Yoneyama, T. Murakami, H. Kimura and A. Inoue: *Ceram. Trans.*, **198** (2006) 109-115.
8) D. V. Louzguine-Luzgin, G. Xie, T. Tsumura, K. Nakata, Y. Murakami, H. M. Kimura and A. Inoue: *Ceram. Trans.*, **198** (2006) 3-8.
9) D. V. Louzguine-Luzgin, G. Q. Xie, T. Tsumura, H. Fukuda, K. Nakata, H. M. Kimura and A. Inoue: *Mater. Sci. Eng. B*, **148** (2008) 88-91.
10) Y. Kawahito, T. Terajima, H. Kimura, T. Kuroda, K. Nakata, S. Katayama and A. Inoue: *Mater. Sci. Eng. B*, **148** (2008) 105-109.